

Analytical Methods

Accepted Manuscript



This is an *Accepted Manuscript*, which has been through the Royal Society of Chemistry peer review process and has been accepted for publication.

Accepted Manuscripts are published online shortly after acceptance, before technical editing, formatting and proof reading. Using this free service, authors can make their results available to the community, in citable form, before we publish the edited article. We will replace this *Accepted Manuscript* with the edited and formatted *Advance Article* as soon as it is available.

You can find more information about *Accepted Manuscripts* in the [Information for Authors](#).

Please note that technical editing may introduce minor changes to the text and/or graphics, which may alter content. The journal's standard [Terms & Conditions](#) and the [Ethical guidelines](#) still apply. In no event shall the Royal Society of Chemistry be held responsible for any errors or omissions in this *Accepted Manuscript* or any consequences arising from the use of any information it contains.

1
2
3
4
5
6
7
8
9
10
11
12
13
14

Interface structure and electrochemical sensing properties of nitrogen-doped diamond like carbon film electrode modified with platinum nanoparticles and 4-aminobenzoic acid

Shuang Wang, Jixiang Zhou, Xian Wang and Guocheng Yang*

*School of Chemistry and Life science, Advanced Institute of Materials Science,
Changchun University of Technology, Changchun 130012, P. R. China*

15
16

Abstract

17
18
19
20
21
22
23
24
25
26
27
28
29
30
31
32
33
34
35
36
37
38

Platinum nanoparticles (PtNPs) and 4-aminobenzoic acid (4-ABA) were applied to modify nitrogen-doped diamond like carbon (N:DLC) film electrode by electrodeposition and cyclic voltammetry. The bare, PtNPs-, 4-ABA-, 4-ABA/PtNPs alternately-modified N:DLC film electrodes were obtained, respectively. Various analysis technologies, such as atomic force microscopy, X-ray photoelectron spectroscopy and micro-Raman spectroscopy, have been used to study surface morphology, chemical composition and bonding structure of the film electrodes. Linear sweep voltammetry and electrochemical impedance spectroscopy were performed to study the relationship between interface structure of chemically modified N:DLC film electrodes and electrochemical sensing properties toward hydrazine sulfate. Acquired results indicate that the different outermost layer modified by 4-ABA or PtNPs behaved differently.

39
40
41
42

Keywords: Interface structure; electrochemical sensing properties; nitrogen-doped diamond like carbon film; platinum nanoparticles; 4-aminobenzoic acid

43
44

1. Introduction

45
46
47
48
49
50
51
52
53
54
55
56
57

Over the years, detection of biological molecules and improvement of electrochemical sensing interface exert a tremendous fascination on researchers in analytical chemistry field. Hydrazine sulfate is a sort of cancerogenic compound,¹⁻³ not only do it harm the health of people who touch it directly or indirectly, but also pollute the environment. When hydrazine sulfate is mixed with air to a certain proportion, it even can trigger explosion. Therefore it is crucial to seek an appropriate method to determine its content accurately. Analytical techniques include ion

58
59
60

* Corresponding author: Tel: +86-431-89399986; fax: +86-431-89399986. E-mail: ychenguo@yahoo.com.

1
2
3 chromatograph, gas chromatography-mass spectrometry, high performance liquid
4 chromatography, fluorescence detection, colorimetric, capillary electrophoresis and
5 electrochemical methods.⁴⁻¹⁵ Among them, electrochemical method is favored by a
6 host of researchers due to its fast response, low cost, high sensitivity, simple operation
7 and excellent reproducibility.
8
9

10
11
12 As we all know, pure diamond itself is nonconductive. Electric insulativity
13 makes its application being limited in electrochemistry. As always, researchers mainly
14 tried to optimize existing method to produce a sort of amorphous carbon with
15 significant sp^3 bonding, which was firstly named diamond like carbon (DLC) by
16 Aisenberg and Chabot.¹⁶ DLC films not only inherit the excellent properties of
17 diamond, but also own a series of advantages such as favorable optical performance,
18 good chemical resistance, and biological compatibility.¹⁷⁻²⁰ However, DLC is a
19 semiconductor which has a band gap. In order to develop the electrical conductivity of
20 DLC, the concept of doping metals or nonmetals was investigated quite intensively in
21 recent years. Nitrogen-doped DLC (N:DLC) is one of the nonmetal-doped DLC films.
22 Due to its admirable quality, N:DLC films have been applied in a wide field of
23 mechanical, optical, electronics and electroanalysis.²¹⁻²⁵ As the electrode material,
24 N:DLC films possess quite a few quintessential virtues with a wide electrochemical
25 potential window, low background current and good electrochemical sensing
26 behavior.²⁶⁻²⁸ What's more, its production condition is comparably mild comparing to
27 those of highly boron-doped diamond (BDD).^{30,31}
28
29
30
31
32
33
34
35
36
37
38
39
40
41
42

43 In this work, the PtNPs, 4-aminobenzoic acid (4-ABA) and 4-ABA/PtNPs
44 alternately-modified N:DLC film electrodes were employed to detect hydrazine
45 sulfate, respectively. The physical and chemical properties related to the surface of
46 bare and modified N:DLC films were characterized by atomic force microscopy
47 (AFM), electrochemical impedance spectroscopy (EIS), X-ray photoelectron
48 spectroscopy (XPS), micro-Raman spectroscopy and electrochemical measurements.
49
50
51
52
53

54 **2. Experimental**

55 **2.1 Materials**

56 4-ABA, $H_2PtCl_6 \cdot 6H_2O$ and hydrazine sulfate were obtained from Sigma-Aldrich
57
58
59
60

1
2
3 and used as received. N:DLC was obtained from RiteDia Corporation. All solutions
4 were made from analytical grade chemicals and Milli-Q ultrapure water (18.25 M Ω
5 cm). The buffer solution of pH 7.0 was prepared from Na₂HPO₄ and NaH₂PO₄
6 containing 0.1 M KCl as supporting electrolytes.
7
8

9 10 11 **2.2 Instrumentation**

12 Electrochemical workstation (CHI852C, Shanghai CH Instruments, China)
13 equipped with a personal computer was used for electrochemical measurements and
14 treating data. The surface morphology of the bare and modified N:DLC films was
15 investigated by AFM (Digital InstrumentsS-3000, Veeco, USA). The EIS was
16 performed with an advanced electrochemical system (PARSTAT 2273, Ametek,
17 America) at room temperature. The bonding structure and chemical composition of
18 the films were measured by XPS (Kratos Axis Ultra, England) with a monochromatic
19 Al K α X-ray radiation (h ν 1486.71 eV). The bond structure of the films was also
20 detected through micro-Raman spectroscopy (RW1000, Renishaw, England) with a
21 He-Ne (632 nm) laser over the range of 800–2000 cm⁻¹. The conventional
22 three-electrode system was used throughout. A bare or a modified N:DLC film was
23 served as the working electrode, a twisted platinum wire as the auxiliary electrode and
24 an Ag/AgCl electrode (KCl saturated) as the reference electrode. All electrode
25 potentials were reported with respected to Ag/AgCl electrode in this paper.
26
27
28
29
30
31
32
33
34
35
36
37
38

39 40 **2.3 Electrodes preparation**

41 A variety of deposition methods (chemical or physical deposition, ion-sputtering,
42 cathodic arc et al) were used to produce N:DLC films.^{17,33} The preparation process of
43 N:DLC thin films used in this work can be described as the following. Employing a
44 pure graphite target (99.95% C) as the carbon source, N:DLC thin films were
45 deposited on conductive n-Si (100) substrates (0.001–0.0035 Ω cm) through a filtered
46 cathodic vacuum arc deposition process. To remove oxide layers and impurities of
47 surface, the Si substrates were etched by pure Ar plasma when the pressure of the
48 vacuum chamber was lowered to ca 2 \times 10⁻⁶ Torr. During deposition, 10-sccm nitrogen
49 (99.999%) was continuously introduced into the vacuum chamber and an arc was
50 ignited by contacting the graphite anode against the graphite target (cathode), thus
51
52
53
54
55
56
57
58
59
60

1
2
3
4
5
6
7
8
9
10
11
12
13
14
15
16
17
18
19
20
21
22
23
24
25
26
27
28
29
30
31
32
33
34
35
36
37
38
39
40
41
42
43
44
45
46
47
48
49
50
51
52
53
54
55
56
57
58
59
60

producing mixed plasma of carbon and nitrogen passing through a double-bend off-plane filter and leading to a N:DLC film deposited on the substrate. A fixed-pulse voltage of 800 V was performed throughout all the depositions. By means of controlling the deposition time, the N:DLC films with a thickness of 100 nm were obtained.^{32–35}

PtNPs-, 4-ABA- and 4-ABA/PtNPs alternately-modified N:DLC film electrodes were obtained by electrochemical deposition and cyclic voltammetry. PtNPs was electrodeposited on GCE by a potentiostatic process at -0.2 V for 360 s in 0.1 M H_2SO_4 aqueous solution containing 1 mM H_2PtCl_6 . 4-ABA/N:DLC film electrode was produced in 0.1 M KCl aqueous solution containing 5 mM 4-ABA via cyclic voltammetry. The potential was set from 0.5 to 1.2 V at 100 mV s^{-1} for 5 cycles.

2.4 Procedure for electrochemical detecting hydrazine sulfate

The bare or modified N:DLC film electrodes were used to sense hydrazine sulfate. A 0.1 M Na_2HPO_4 - NaH_2PO_4 aqueous solution (4 mL) containing a specific amount of hydrazine sulfate of 10 mM was added to the electrochemical cell. The linear sweep voltammograms of hydrazine sulfate on the electrodes were recorded in the potential from 0.0 to 1.0 V at a scan rate of 100 mV s^{-1} .

3. Results and discussion

3.1 Electrode modification and characterization

Fig. 1 shows modification process of PtNPs and 4-ABA on N:DLC films. In Fig. 1A, when the deposition time is about 100 s, the current almost maintains steady, this indicates the formation of PtNPs layer on GCE. The deposition time of 360 s is enough to get a stable PtNPs/N:DLC film electrode. The cyclic voltammograms of 4-ABA on N:DLC film was shown in Fig. 1B. There is an irreversible oxidation peak at about 1.05 V in the first cycle; this oxidation peak disappears with the increasing of scan cycles. This manifests that the surface of N:DLC has been modified by the 4-ABA layer.³⁶ Combing electrochemical deposition with cyclic voltammetry, the 4-ABA/PtNPs alternately-modified N:DLC film electrode also can be prepared successfully.

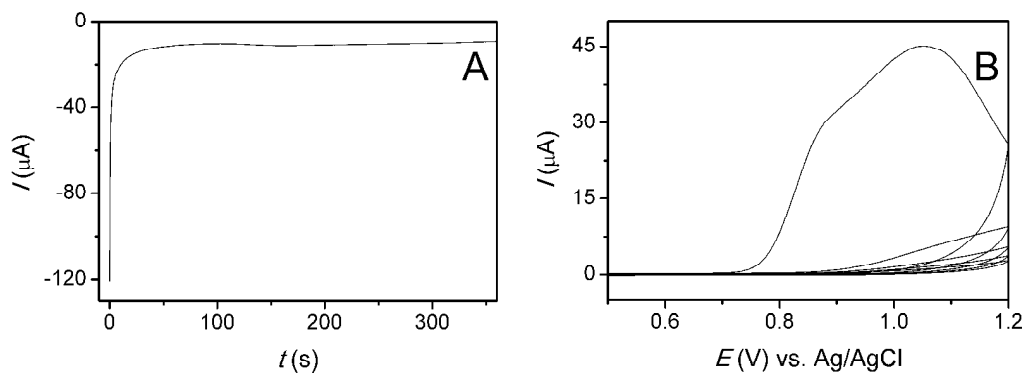


Fig. 1. The modification process of PtNPs (A) and 4-ABA (B) on N:DLC films.

The surface morphology of the bare and modified N:DLC films were investigated by AFM using a Si_3N_4 cantilever which was operated in a tapping mode with a scan size of $5 \mu\text{m} \times 5 \mu\text{m}$. An average surface roughness value was taken by measuring five times on each sample. The root-mean-square (RMS) roughness of the bare (A), 4-ABA- (B), PtNPs- (C), 4-ABA/PtNPs (D) alternately-modified N:DLC films are 0.68, 1.71, 87.34 and 59.61 nm, respectively. Fig. 2A shows that the AFM images of the bare N:DLC film, which is presented as a woolen carpet.³⁷ After 4-ABA was decorated, the woolen carpet was transformed to ice falls, as revealed in Fig. 2B. Fig. 2C displays that the N:DLC coated by PtNPs, which looks like the stone forests. Discovered through comparative analysis, the surface coverage of PtNPs-modified N:DLC film is not as compact as the N:DLC film modified by 4-ABA. The last one showed in Fig. 2D seems like a cauliflower. It was modified by 4-ABA and PtNPs alternately and possessed the surface property of the both.³⁸

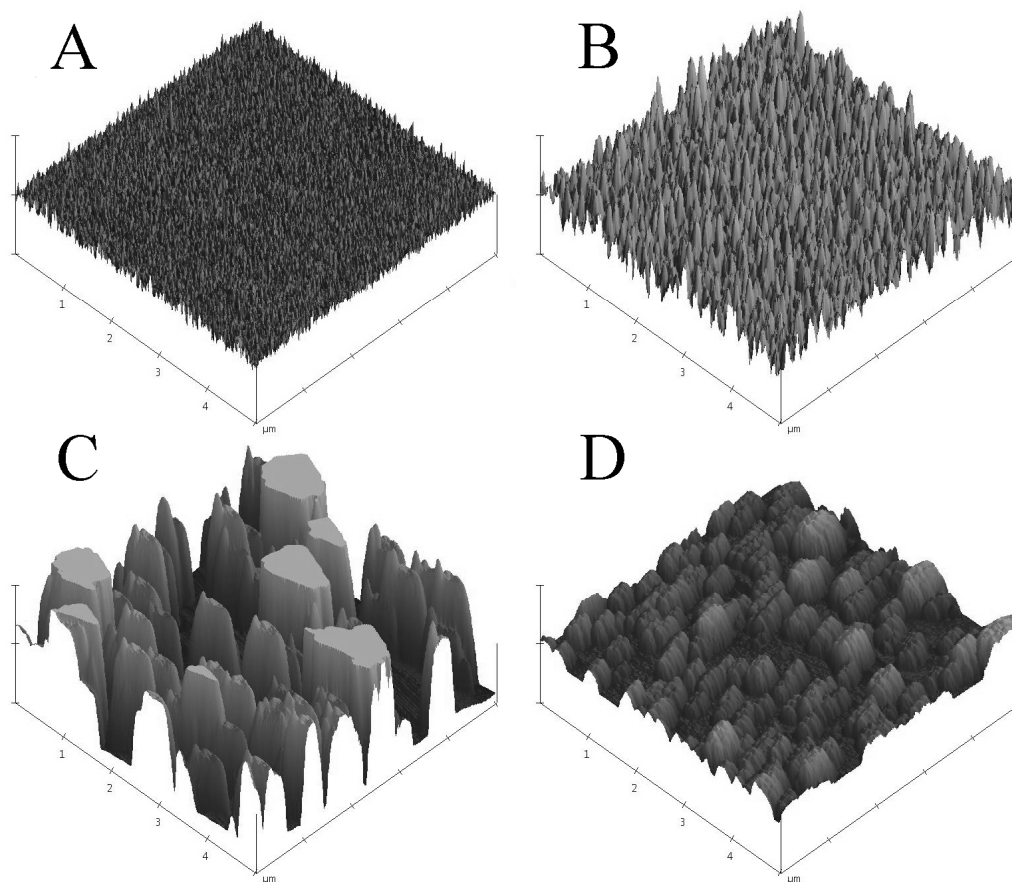


Fig. 2. AFM images of the bare N:DLC (A), 4-ABA-modified N:DLC (B), PtNPs-modified N:DLC (C), 4-ABA/PtNPs alternately-modified N:DLC (D).

XPS is an effective and non-destructive technique to investigate the chemical composition and structure of carbon materials. In this work, a wide scan range from 0 eV to 1200 eV was employed. An overview of all elements was provided by the binding energy of bare and modified N:DLC film. Fig. 3 exhibits the determination signals deprived from the elements of O, C, N and Pt. From Fig. 3A it can be seen that the peak of O 1s is at around 531.3 eV which was attributed to the oxidation of the N:DLC film surface.³⁹ Fig. 3B demonstrates that the peaks of C 1s, N–N sp² and sp³ approximately appeared at 284.6 eV, 284.5 eV and 286.2 eV, respectively. The peak at about 287.3 eV certificated the formation of C–N bonding. Fig. 3C reveals that the N 1s, N–N sp² and sp³, and N–O peaks are separately at 390.4 eV, 390.2 eV, 400.0 eV and 402.2 eV.⁴⁰ In Fig. 3D, the characteristic peaks at about 75.9 eV and 72.3 eV manifest the presence of Pt 4f_{5/2} and Pt 4f_{7/2}. It also can be seen that the Pt⁰ and Pt⁴⁺ of

Pt 4f components were located at cal 72.1 eV and 73.7 eV, respectively. The existence of such elements characterize the structure of the bare N:DLC and N:DLC modified by PtNPs.

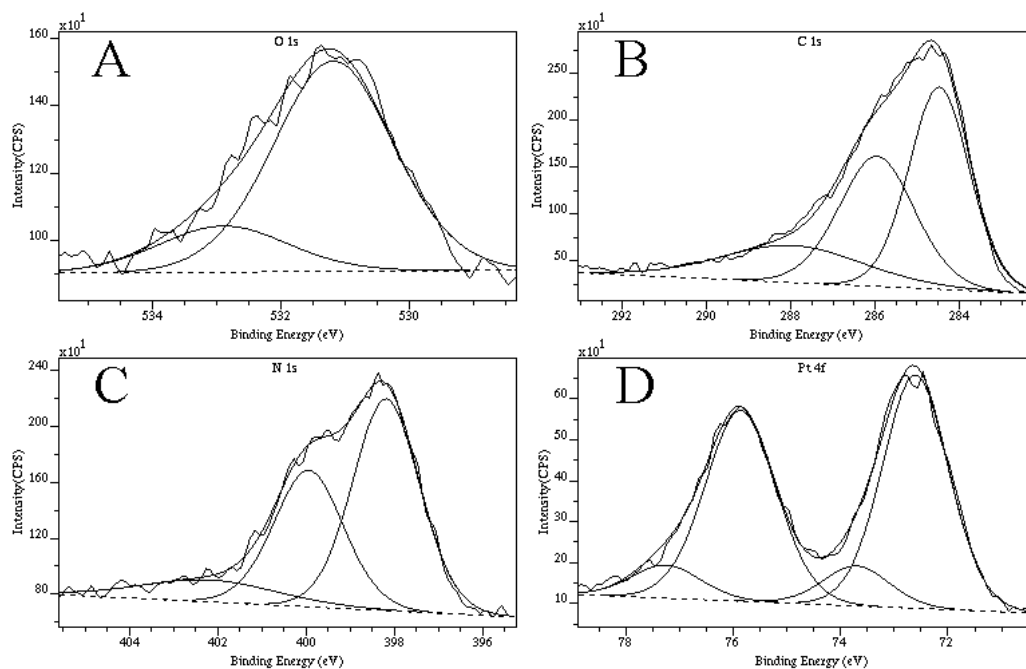


Fig. 3. XPS results of O 1s (A), C 1s (B) and N 1s (C) peaks of the N:DLC film, Pt 4f (D) peak of Pt₄₀₀/N:DLC films.

With regard to the measurement of defects and disordered structures, Raman spectroscopy is the most efficient technology. Fig. 4 presents the micro-Raman spectrum of the N:DLC film, which displays the G band and D band in N:DLC film. The G and D bands represent stretching vibration in-plane of the graphitic sp²-based carbon and the lattice defects of carbon atom. The peaks of the G and D bands are located at 1563 cm⁻¹ and 1380 cm⁻¹, respectively.⁴¹ The intensity of the I_D/I_G ratio is about 1.48, this value indicates that the carbon atom of sp² hybridization is higher than that of sp³ hybridization. And the higher the I_D/I_G ratio is, the more the lattice defects exist.⁴²

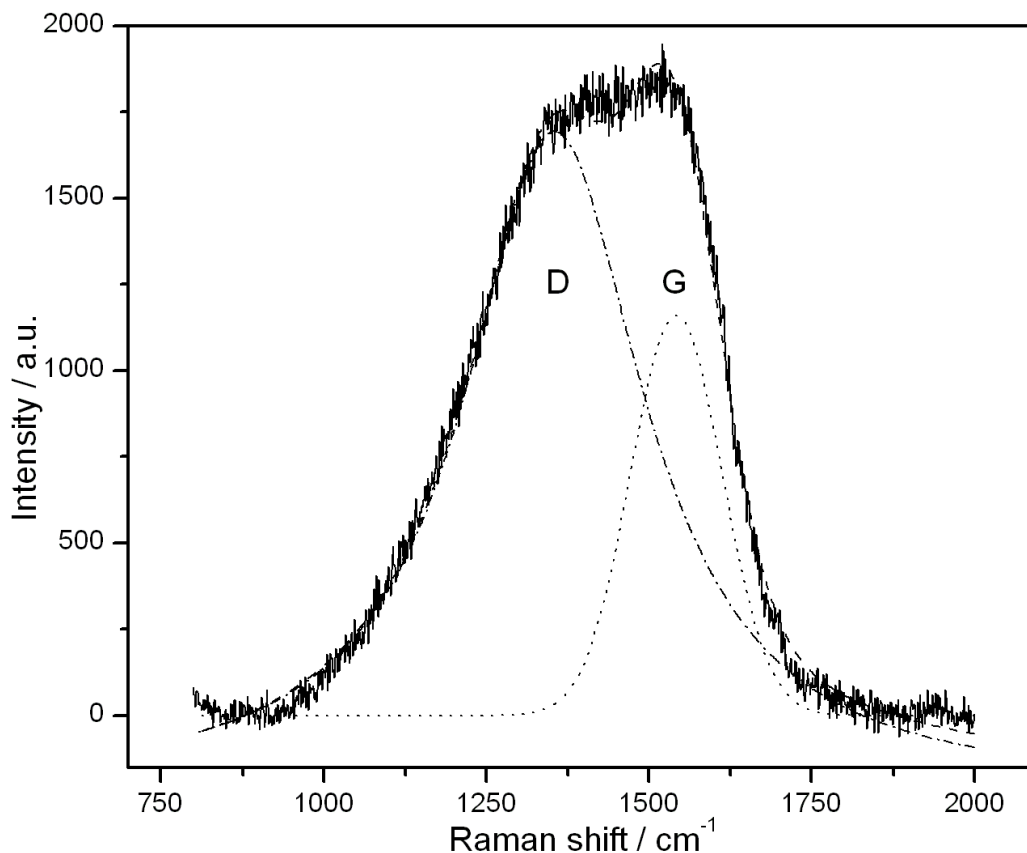


Fig. 4. The micro-Raman spectrum of the N:DLC film

Fig. 5 shows that the impedance diagrams of the bare and modified N:DLC films. The left column of Fig. 5 displays that the PtNPs as outermost layer were modified on N:DLC film, while the right column represents the outermost layer was grafted by 4-ABA. On the whole, the radius of first semicircle is bigger, but the second is smaller with increasing the layer numbers in the left column. The first semicircle is controlled by the polarization resistance, which is also called intramembraneous resistance.⁴³ The second semicircle is attributed to the resistance related to the redox reaction of probes. Fig. 6 shows the relationship between the resistance and layer numbers of 4-ABA/N:DLC (A) and PtNPs/N:DLC (B). With the layer numbers increasing, the intramembraneous resistance was growing. The conclusion is also in accordance with the resistance of redox reaction in right column. The variation trend of the resistance is decreasing at first, and then increasing, finally decreasing. The resistance seems unlike owing to its different conductivity. As a sort of metal NPs, PtNPs possess excellent conductivity. The conductivity of N:DLC modified by

4-ABA is other than that by PtNPs. A conclusion can be made that when the N:DLC was alternately coated by PtNPs and 4-ABA, the impedance performance of the modified N:DLC film was controlled by the outermost layer. This result is also suitable for 4-ABA/N:DLC film electrodes. With the increasing of the layer numbers, the electron-transfer resistance is enlarging. It implies that the solid electrolyte interphase layer is more and more stable.

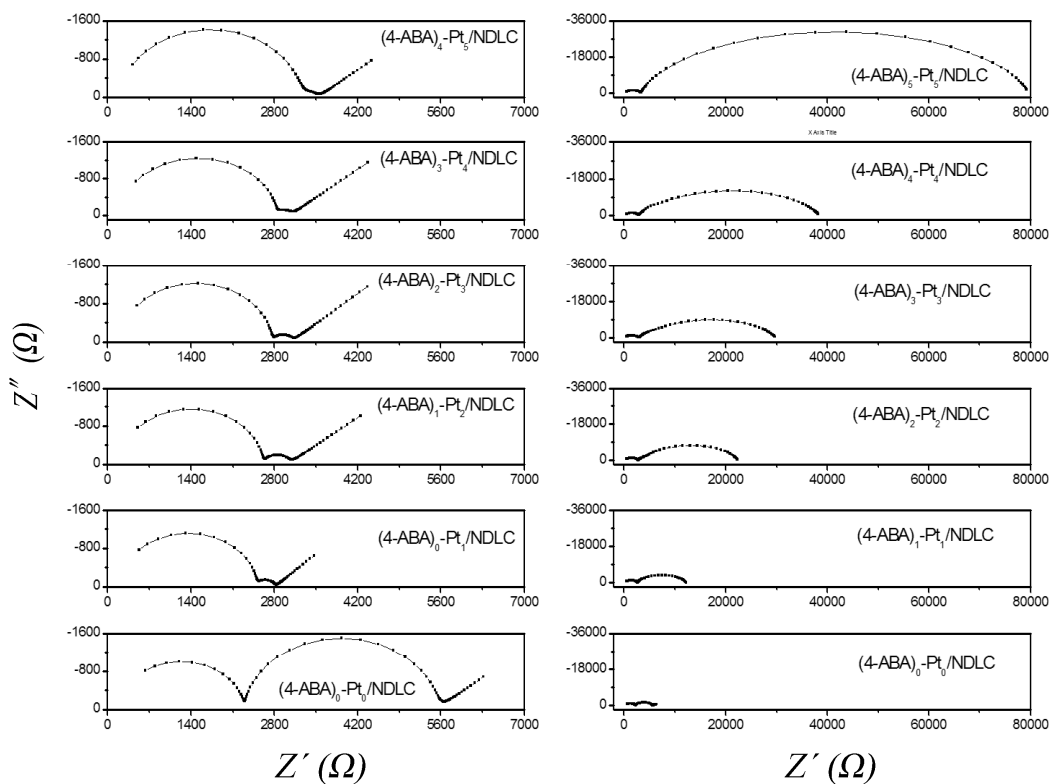


Fig. 5. The Nyquist plots of the bare N:DLC film and N:DLC alternately coated by PtNPs and 4-ABA with different layer numbers (the number in the right bottom corner of modifiers represents the layer numbers) in 0.1 M KCl solution containing 5 mM $\text{Fe}(\text{CN})^{3-/4-}$.

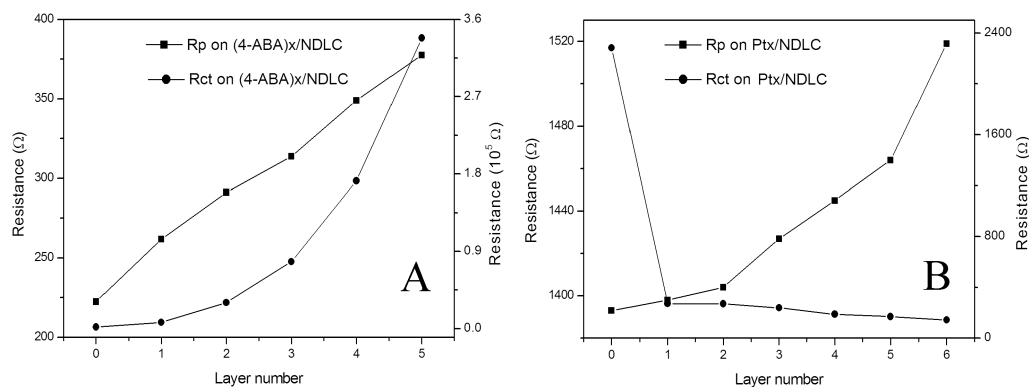


Fig. 6. The relationship between the resistance and layer numbers of 4-ABA/N:DLC (A) and PtNPs/N:DLC (B).

3.2 Electrochemical sensing properties of the electrodes

Different electrochemical sensing properties were controlled by different geometric and electronic structures of surface.⁴⁴⁻⁴⁶ Fig. 7 shows linear sweep voltammograms of the bare, PtNPs-, 4-ABA-, 4-ABA/Pt alternately-modified N:DLC films in different concentrations of $\text{N}_2\text{H}_4 \cdot \text{H}_2\text{SO}_4$ at a scan rate of 100 mV s^{-1} . From Fig. 7A it can be seen that the currents are increasing with adding $\text{N}_2\text{H}_4 \cdot \text{H}_2\text{SO}_4$ successively. While the electrode which was modified by PtNPs behaved differently from the bare N:DLC electrode. Its current response is too little to recognize. That is because the PtNPs-modified N:DLC looks like a stone forest, its effective surface area called active sites is less. Therefore its sensing performance was not satisfied. From Figs. 7C and D we can see that there are two peaks enlarging as the increasing of the $\text{N}_2\text{H}_4 \cdot \text{H}_2\text{SO}_4$ concentration. However the heights of the left peak at around 0.72 V and the right at about 0.84 V are diverse. The height of the left peak at around 0.72 V is higher than the right at about 0.84 V, as shown in Fig. 7C, but the phenomenon in Fig. 7D is exactly opposite. Obtained results prove that 4-ABA/PtNPs alternately-modified N:DLC films possess an outstanding property of both the 4-ABA/N:DLC and PtNPs/N:DLC film electrodes for sensing $\text{N}_2\text{H}_4 \cdot \text{H}_2\text{SO}_4$, therefore the peak at around 0.84 V was attributed to the mutual detection of the PtNPs and 4-ABA. From Figs. 7C and D it can be seen that there are two background peaks respectively at 0.2 V and 0.8 V without adding $\text{N}_2\text{H}_4 \cdot \text{H}_2\text{SO}_4$. The peaks are attributed to the modified layer itself which was oxidized in buffer solution. When a certain concentration of $\text{N}_2\text{H}_4 \cdot \text{H}_2\text{SO}_4$

was added in the electrochemical cell, the environment of detection was also changed. Consequently background current was decreasing and disappeared finally. With a continued addition of $N_2H_4 \cdot H_2SO_4$, the electrochemical signal was enhancing.

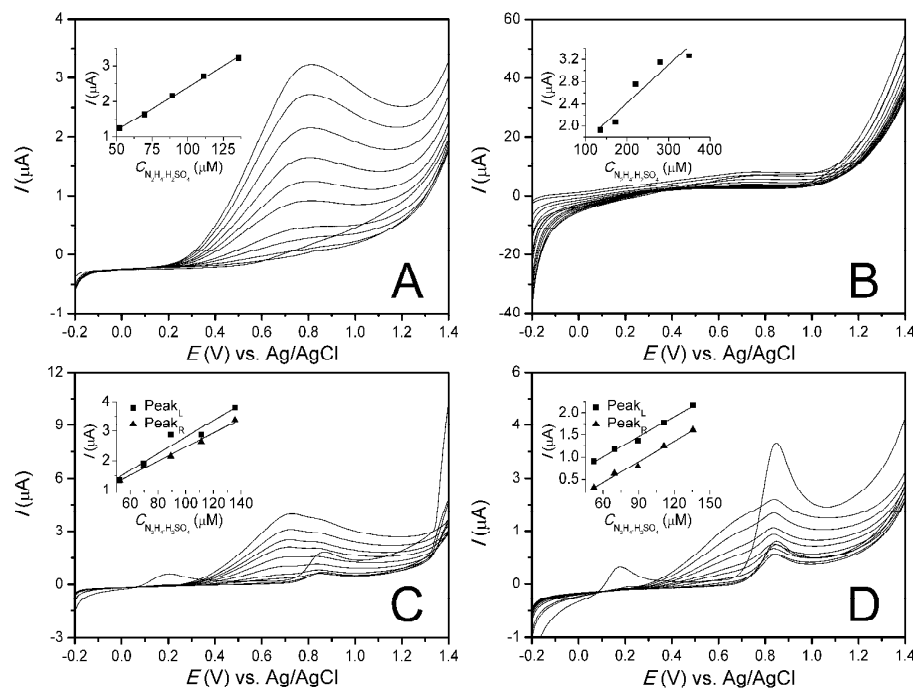


Fig. 7. Linear sweep voltammograms of the bare (A), PtNPs- (B), 4-ABA- (C), 4-ABA/PtNPs (D) alternately-modified N:DLC films in different concentrations of $N_2H_4 \cdot H_2SO_4$ at a scan rate of 100 mV s^{-1} .

Table 1. The parameter of the linear regression equation for the electrodes

Electrodes	Parameters		R	LOD (μM)	Liner range	
	k ($\mu\text{A}/\mu\text{M}$)	b (μA)				
Bare N:DLC	0.0240	-0.0054	0.9976	7.6636	15 μM -0.35mM	
PtNPs/N:DLC	0.00682	1.0557	0.8820	125.787	110 μM -0.35mM	
4-ABA/N:DLC	P _L	0.0278	0.0044	0.9211	4.6064	15 μM -0.35mM
	P _R	0.0236	0.1034	0.9891	65.6562	25 μM -0.35mM
4-ABA-PtNPs/N:DLC	P _L	0.0151	0.0994	0.9893	16.5554	25 μM -0.35mM
	P _R	0.0154	-0.4882	0.9825	39.7442	37 μM -0.35mM

The data shows that the correlations of the linear regression equation related to the bare N:DLC, 4-ABA/N:DLC and 4-ABA/PtNPs alternately-modified N:DLC are very good. This indicates that the 4-ABA/PtNPs alternately-modified N:DLC film is other than PtNPs/N:DLC, which possess very stable electrochemical sensing properties toward $\text{N}_2\text{H}_4 \cdot \text{H}_2\text{SO}_4$ in neutral solution. In addition, the limit of detection (LOD) of $\text{N}_2\text{H}_4 \cdot \text{H}_2\text{SO}_4$ on the bare and modified N:DLC electrodes was also calculated according to 3σ method⁴⁷

$$\text{LOD} = \frac{3s_{\text{bl}}}{k} = 3\sigma \quad (1)$$

where s_{bl} is the standard deviation of the peak currents of the blank ($n = 5$), and k is the slope of the calibration curve as shown in Table 1.

4. Conclusion

In this work, the 4-ABA-, PtNPs- and 4-ABA/PtNPs alternately-modified N:DLC electrodes were successfully prepared via a simple electrochemical deposition and oxidation method. Various characterizations and electrochemical measurements show that different film structure strongly affect the sensing performance for electrooxidizing $\text{N}_2\text{H}_4 \cdot \text{H}_2\text{SO}_4$. Consequently, the special property for detecting $\text{N}_2\text{H}_4 \cdot \text{H}_2\text{SO}_4$ can be realized through the construction of composite structure. Further optimization of the work will continue to be investigated by our group.

Acknowledgements

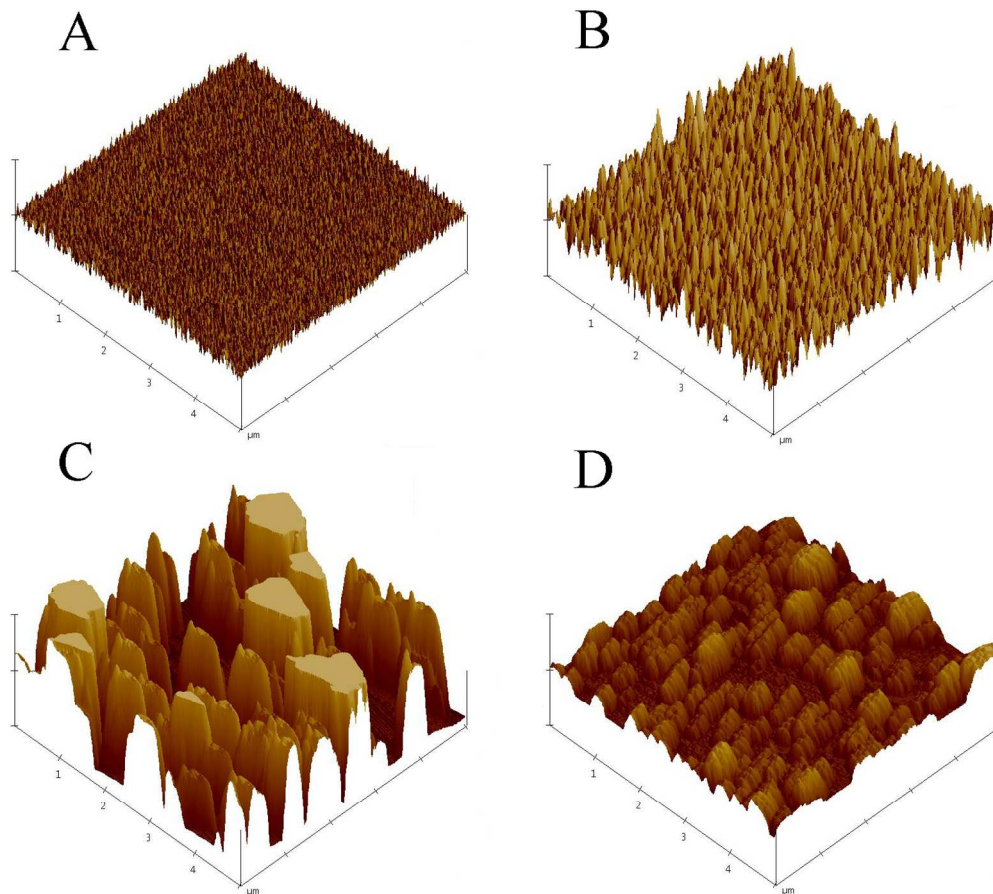
This work was supported by the National Natural Science Foundation of China (Nos. 21005008 and 51374040); SRF for ROCS, SEM (No. 20111568-2); High-level Innovation and Entrepreneurship Talent Program, Jilin Province of China; and the Scientific and Technical Innovation and Entrepreneurship Project for Returned Overseas Chinese Scholars, Jilin Province of China (No. 201129).

References

- [1] C. Merusi, C. Corradini, A. Cavazza, C. Borromei and P. Salvadeo, *Food Chem.*, 2010, **120**, 615.
- [2] C. Ait Ramdane-Terbouche, A. Terbouche, S. Djebbar and D. Hauchard, *Talanta*, 2014, **119**, 214.
- [3] Y. Tan, J. Yu, J. Gao, Y. Cui, Y. Yang and G. Qian, *Dyes Pigments*, 2013, **99**, 966.
- [4] P. Niedzielski, I. Kurzyca and J. Siepak, *Anal. Chim. Acta*, 2006, **577**, 220.
- [5] N. Wang, R.Q. Wang and Y. Zhu, *J. Hazard. Mater.*, 2012, **235–236**, 123.
- [6] M. Akyuz, S. Ata, *Talanta*, 2009, **79**, 900.
- [7] D. Tsikas, *Analyst*, 2011, **136**, 979.
- [8] S. Goswami, S. Paul, A. Manna, *RSC Adv.*, 2013, **3**, 18872.
- [9] H. Kodamatani, S. Yamazaki, K. Saito, T. Tomiyasu and Y. Komatsu, *J. Chromatogr. A*, 2009, **1216**, 3163.
- [10] B. Zargar, A. Hatamie, *Sens. Actuators B: Chem.*, 2013, **182**, 706.
- [11] C.M. Rushworth, Y. Yogarajah, Y. Zhao, H. Morgan and C. Vallance, *Anal. Methods*, 2013, **5**, 239.
- [12] T. Y. You, L. Niu, J. Y. Gui, S. J. Dong and E. K. Wang, *J. Pharm. Biomed. Anal.*, 1999, **19**, 231.
- [13] X. Chen, W. Liu, L. Tang, J. Wang, H. Pan and M. Du, *Mater. Sci. Eng. C*, 2014, **34**, 304.
- [14] P. F. Pereira, M. C. Marra, A. B. Lima, W. T. P. dos Santos, R. A. A. Munoz and E. M. Richter, *Diamond Relat. Mater.*, 2013, **39**, 41.
- [15] Y. Li, S. Feng, S. Li, Y. Zhang and Y. Zhong, *Sens. Actuators B: Chem.*, 2014, **190**, 999.
- [16] J. Robertson, *Mater. Sci. Eng. R*, 2002, **37**, 129.
- [17] J. Liu, X. Wang, B.J. Wu, T.F. Zhang, Y.X. Leng and N. Huang, *Vacuum*, 2013, **92**, 39.
- [18] P. W. Shum, Z. F. Zhou and K. Y. Li, *Tribol. Int.*, 2013, **65**, 259.
- [19] M. H. Ahmed, J. A. Byrne, J. A. D. McLaughlin, A. Elhissi and W. Ahmed, *Appl. Surf. Sci.*, 2013, **273**, 507.

- 1
2
3
4 [20] U. Depner-Miller, J. Ellermeier, H. Scheerer, M. Oechsner, K. Bobzin, N.
5 Bagcivan, T. Brögelmann, R. Weiss, K. Durst and C. Schmid, *Surf. Coat. Technol.*,
6 2013, **237**, 284.
7
8
9 [21] L. Yang, A. Neville, A. Brown, P. Ransom and A. Morina, *Tribol. Int.*, 2014, **70**,
10 26.
11
12 [22] H. Abdullah Tasdemir, M. Wakayama, T. Tokoroyama, H. Kousaka, N. Umehara
13 and Y. Mabuchi, T. Higuchi, *Wear*, 2013, **307**, 1.
14
15 [23] G. Dai, F. Pohlenz, A. Felgner, H. Bosse and H. Kunzmann, *CIRP Ann. Manuf.*
16 *Techn.*, 2013, **62**, 543.
17
18 [24] W. Tillmann, E. Vogli and F. Hoffmann, *Surf. Coat. Technol.*, 2009, **204**, 1040.
19
20 [25] A. S. Hamdy, *Electrochim. Acta*, 2011, **56**, 1554.
21
22 [26] J. K. Lee, W. Y. Yoon and B. K. Kim, *J. Electrochem. Soc.*, 2013, **160**, A1348.
23
24 [27] A. A. Arie, J. K. Lee, *Diamond Relat. Mater.*, 2011, **20**, 403.
25
26 [28] D. Hofmann, S. Kunkel, K. Bewilogua and R. Wittorf, *Surf. Coat. Technol.*, 2013,
27 **215**, 357.
28
29 [29] X. F. Liu, J. B. Pu, L. P. Wang and Q. J. Xue, *J. Mater. Chem. A*, 2013, **1**, 3797.
30
31 [30] R. Bogdanowicz, J. Czupryniak, M. Gnyba, J. Ryl, T. Ossowski, M. Sobaszek, E.
32 M. Siedlecka and K. Darowicki, *Sens. Actuators B: Chem.*, 2013, **189**, 30.
33
34 [31] R. F. Brocenschi, R. C. Rocha-Filho, L. Li and G. M. Swain, *J. Electroanal.*
35 *Chem.*, 2014, **712**, 207.
36
37 [32] T. Kamata, D. Kato, S. Hirono and O. Niwa, *Anal. Chem.*, 2013, **85**, 9845.
38
39 [33] X. Yang, L. Haubold, G. DeVivo and G. M. Swain, *Anal. Chem.*, 2012, **84**, 6240.
40
41 [34] L. C. Cheng, T. F. Hung, P. H. Lee, I. C. Lin, H. L. Wen, L. H. Lu, C. L. Chiu, S. C.
42 Chen, J. C. Sung, B. J. Weng and R. S. Liu, *RSC Adv.*, 2013, **3**, 5917.
43
44 [35] N. Menegazzo, M. Kahn, R. Berghauser, W. Waldhauser and B. Mizaikoff,
45 *Analyst*, 2011, **136**, 1831.
46
47 [36] G. C. Yang, L. Wang, J. B. Jia, D. F. Zhou, D. F. Li, *J. Solid State Electrochem.*,
48 2012, **16(9)**, 2967.
49
50 [37] D. Bootkul, B. Supsermpol, N. Saenphinit, C. Aramwit and S. Intarasiri, *Appl.*
51 *Surf. Sci.*, 2014, **310**, 284.
52
53
54
55
56
57
58
59
60

- 1
2
3 [38] H. Nakazawa, R. Kamata and S. Okuno, *Diamond Relat. Mater.*, 2015, **51**, 7.
4
5 [39] L. C. Cheng, T. F. Hung, P. H. Lee, I. C. Lin, H. L. Wen, L. H. Lu, C. L. Chiu, S.
6
7 C. Chen, J. C. Sung, B. J. Weng and R. S. Liu, *RSC Adv.*, 2013, **3**, 5917.
8
9 [40] L. Zhang, Z. Su, F. Jiang, L. Yang, J. Qian, Y. Zhou, W. Li and M. Hong,
10
11 *Nanoscale*, 2014, **6**, 6590.
12
13 [41] R. Bresciani, S. Marzorati, A. Lascialfari, B. Sacchi, N. Santo and M. Longhi,
14
15 *Electrochem. Commun.*, 2015, **51**, 27.
16
17 [42] S. C. Ray, W. Mbiombi and P. Papakonstantinou, *Curr. Appl. Phys.*, 2014, **14**,
18
19 1845.
20
21 [43] A. J. Jeevagan and S. A. John, *RSC Adv.*, 2013, **3**, 2256.
22
23 [44] A. Safavi and M. Tohidi, *Anal. Methods*, 2012, **4**, 2233.
24
25 [45] R. S. Das, B. Singh, R. Banerjee and S. Mukhopadhyay, *Dalton T.*, 2013, **42**,
26
27 4068.
28
29 [46] A. Gurlo, *Nanoscale*, 2011, **3**, 154.
30
31 [47] C. Xu, H. Cai, P. G. He and Y. Z. Fang, *Analyst*, 2001, **126**, 62.
32
33
34
35
36
37
38
39
40
41
42
43
44
45
46
47
48
49
50
51
52
53
54
55
56
57
58
59
60



565x508mm (72 x 72 DPI)

1
2
3
4
5
6
7
8
9
10
11
12
13
14
15
16
17
18
19
20
21
22
23
24
25
26
27
28
29
30
31
32
33
34
35
36
37
38
39
40
41
42
43
44
45
46
47
48
49
50
51
52
53
54
55
56
57
58
59
60